Cleavage of the C-Terminal Serine of Human αA-Crystallin Produces αA_{1-172} with Increased Chaperone Activity and Oligomeric Size†

Atya Aziz,‡ Puttur Santhoshkumar,§ Krishna K. Sharma,§ and Edathara C. Abraham*,‡

Department of Biochemistry and Molecular Biology, University of Arkansas for Medical Sciences, Little Rock, Arkansas 72205, and Department of Ophthalmology, University of Missouri, Columbia, Missouri 65212

Received September 8, 2006; Revised Manuscript Received November 13, 2006

ABSTRACT: This study aimed to study the oligomeric size, structure, hydrodynamic properties, and chaperone function of the C-terminally truncated human αA-crystallin mutants with special emphasis on αA_{1-172} which is the cleavage product of the $Ser_{172}-Ser_{173}$ bond, unique to human lenses and constituting a major part of αA-crystallin. Various truncated forms of human αA-crystallins were prepared by site-directed mutagenesis. The proteins were expressed in *Escherichia coli* BL21(DE3) pLysS cells and purified by size exclusion column chromatography. Molecular masses and the other hydrodynamic properties were determined by dynamic light scattering measurements. The secondary and tertiary structural changes were assessed by far- and near-UV CD spectra measurements, respectively. Chaperone activity was determined by using ADH, insulin, and βL-crystallin as the target proteins. αA_{1-172} exhibited a significant increase in oligomeric size, i.e., 866 kDa by light scattering measurements as compared to 702 kDa in αA-wt. αA_{1-172} and αA-wt had similar secondary structure, but the former exhibited slightly altered tertiary structure. The most interesting observation was that αA_{1-172} behaved as a 28−46% better chaperone than αA-wt. The oligomeric size and structure of αA_{1-168} were similar to those of αA-wt, while the chaperone activity was decreased by 12−23%. αA_{1-162}, on the other hand, had an oligomeric size of 400 kDa, a decrease in chaperone activity of 80−100%, and significantly altered secondary and tertiary structures. The data show that the overall chaperone function of αA-crystallin will be significantly improved by the presence of the major truncated product αA_{1-172}. This will be beneficial to the lens undergoing oxidative stress. Since αA_{1-168} and αA_{1-162} are present only in small amounts, their effect would be minimal.

The human eye lens has a high protein content that is necessary for the lens to maintain its transparency and high refractive index. The crystallins compose approximately 90% of the soluble protein of the vertebrate eye lens and include three major families of ubiquitously expressed crystallins, i.e., α-, β-, and γ-crystallins. The predominant protein component is α-crystallin which constitutes ∼25−50% of the total protein of the lens. The α-crystallin which consists of two types of subunit polypeptides, namely, the αA- and αB-crystallins, is usually isolated as a polydispersed mixture of large heteroaggregates with molecular masses in the range of 300−800 kDa (*1*−*4*). αA and αB subunits, the sequences of which are 57% identical, have molecular masses of ∼20 kDa and contain 173 and 175 amino acid residues, respectively (*5*, *6*). The α-crystallin is no longer considered as a simple structural protein of the vertebrate eye lens since the discovery that α-crystallin belongs to the class of small heat shock proteins (sHsps)[1] and functions as a molecular chaperone, preventing aggregation of partially unfolded proteins (*7*, *8*).

The model structure of α-crystallin is proposed to consist of a globular N-terminal domain and a slightly larger C-terminal domain with an exposed C-terminal arm (*9*). The characteristic C-terminal stretch of 80−100 residues known as the "α-crystallin domain" contains short consensus sequences that are highly conserved in the α-crystallin/small heat shock protein (α-Hsp) superfamily (*4*, *10*, *11*). The N- and C-terminal regions flanking this domain differ considerably in both the sequence and length and are believed to control oligomeric assembly and size (*12*−*14*). The C-terminal extension of 140−173 amino acid residues in αA-crystallin is largely unstructured and contains the flexible, polar, and solvent-exposed C-terminal tail of 8−10 amino acid residues (*10*, *15*−*18*). Previous studies have shown that the flexibility of the C-terminus, a feature shared by mammalian sHsps, is essential for the chaperoning function and thermodynamically stable structure (*19*, *20*).

Cleavage of the amino acid residues in the C-terminal region of αA-crystallin is the major modification occurring

† This work was supported by Grants EY11352 (E.C.A.) and EY009855 (K.K.S.) from the National Institutes of Health.

* To whom correspondence should be addressed: Department of Biochemistry and Molecular Biology, University of Arkansas for Medical Sciences, Slot 516, Little Rock, AR 72205. Phone: (501) 526-6088. Fax: (501) 686-8169. E-mail: ecabraham@uams.edu.

‡ University of Arkansas for Medical Sciences.

§ University of Missouri.

[1] Abbreviations: CD, circular dichroism; HPLC, high-performance liquid chromatography; ADH, alcohol dehydrogenase; EDTA, ethylenediaminetetraacetic acid; SDS−PAGE, sodium dodecyl sulfate−polyacrylamide gel electrophoresis; sHsp, small heat shock protein; BCA, bicinchoninic acid.

10.1021/bi0618722 CCC: $37.00
Published on Web 02/06/2007

to αA-crystallin (*21*−*25*). Removal of C-terminal residues from the flexible C-terminal region has been shown to affect chaperone activity, thus implying that this region is involved in the functional activity of the protein (*26*). The chaperone activity was found to be affected in fetal bovine lens αA-crystallin when 16 residues were cleaved from the C-terminus by limited tryptic digestion (*26*). The cleavage of 11−12 residues from the C-terminal region of rat αA-crystallin by calpain II resulted in a loss of chaperone activity (*27*). Introducing a highly hydrophobic residue in the C-terminal extension resulted in reduced solubility and thermostability of the protein (*28*). Similar results were observed when the deletion of 17 C-terminal residues resulted in a marked loss of chaperone-like activity of the truncated αA-crystallin (*29*). When the C-terminal extension of αA-crystallin was swapped with αB-crystallin, it resulted in the alteration of the structure and function of the proteins (*30*). We have recently reported data regarding the influence on the structure, oligomerization, and chaperone function of various C-terminally truncated αA-crystallins found in rat lenses (*31*). These mutants have been identified as αA_{1-168}, αA_{1-163}, αA_{1-162}, αA_{1-157}, and αA_{1-151}. However, such modifications do not constitute the major form of modification of αA-crystallin in human lenses, although low levels of αA_{1-168} and αA_{1-162} have been detected (*32*).

In human lenses, C-terminal cleavage of αA-crystallin at residues 101, 162, 168, and 172 has been reported (*24*, *33*, *34*). In another study, 13 cleavage sites were found in human α-crystallin, including truncation at C-terminal residues 151, 162, 168, and 172 of αA-crystallin (*32*). The major post-translational modifications found in water soluble human lens crystallins include the loss of the C-terminal Ser residue (*24*, *25*, *32*−*37*). Our previous studies have also shown enhanced cleavage of the C-terminal Ser residue in diabetic human lenses by electrospray ionization mass spectrometry (*36*). The average percentage of the truncated αA_{1-172} mutant in the intact α-crystallin was 30% which increased to nearly 50% in diabetic lenses. Thus, the presence of this mutant is expected to influence the overall chaperone function of αA-crystallin. Takemoto identified and quantitated the Ser_{172}−Ser_{173} bond cleavage product from human lenses of different ages (*37*). The data suggested that the cleavage is an age-dependent event occurring rapidly during the first 12 years of life and slowly thereafter; the cleaved product, αA_{1-172}, reached ∼45% of the total α-crystallin in ∼12 years and ∼50% in 60 years. All the observations given above suggest that the cleavage, particularly at the Ser_{172}−Ser_{173} bond, may play an important role in lens function either in development or in a stress-induced condition like diabetes and aging. This study aims to determine the oligomeric structure, hydrodynamic properties, and chaperone function of the various truncated αA-crystallins which exist in human lenses with a special emphasis on αA_{1-172}.

EXPERIMENTAL PROCEDURES

Cloning, Site-Directed Mutagenesis, and Overexpression of Human αA-Crystallin and the C-Terminally Truncated Mutants. Cloning of human αA-crystallin and subsequent subcloning into the pET-23d(+) expression vector have been described previously (*38*, *39*). To generate the different C-terminally truncated human αA-crystallins lacking 1, 5, and 11 residues, stop codons were introduced at the positions of interest using the Quick Change site-directed mutagenesis kit (Stratagene). Coding sequences for the human αA wild type (αA-wt) and its C-terminally truncated mutants were confirmed by automated DNA sequencing. The overexpression of αA-wt and the truncated mutants (in the pET vector) was achieved in *Escherichia coli* BL21(DE3) pLysS cells. The procedures followed for the expression and purification of the wild-type and truncated proteins have been described in our earlier work (*40*).

Purification of Human αA-Crystallin and the C-Terminally Truncated Mutants. The expressed proteins were purified by size exclusion chromatography on Sephacryl S-300 HR size exclusion columns with dimensions of 1.6 cm × 120 cm. The fractions corresponding to the peak volume were collected and pooled, and the pooled peak fractions were concentrated in an Amicon ultrafiltration unit and repurified by molecular sieve HPLC using a 600 mm × 7.8 mm BIOSEP-SEC 4000 column (Phenomenex) with Beckman HPLC System Gold. The mobile phase was Tris-EDTA buffer (pH-7.4) consisting of 50 mM Tris, 150 mM NaCl, and 10 mM EDTA, and the flow rate was maintained at 1.0 mL/min. Protein concentrations were measured by the BCA method (BCA protein assay reagent; Pierce, Rockford, IL).

SDS−*Polyacrylamide Gel Electrophoresis.* The purity of the wild-type and truncated αA-crystallins was examined by sodium dodecyl sulfate−polyacrylamide gel electrophoresis (SDS−PAGE) according to the method of Laemmli (*41*) under reducing conditions. Electrophoresis was conducted using a 12% separating gel at a constant voltage of 150 V for 2−3 h. Gels were stained with Coomassie Brilliant Blue R-250.

Determination of Quaternary Structural Parameters of Wild-Type αA-Crystallin and Truncated Mutants by Dynamic Light Scattering (DLS). The light scattering measurements of purified αA-wt and its truncated mutants [1 mg/mL protein in 0.1 M PBS buffer (pH 7.4)] were taken with a DLS system from Wyatt Technology (Santa Barbara, CA). In brief, the purified recombinant proteins were incubated at 37 °C for 1 h. Each protein sample (∼100 μg) was injected into a TSK G5000PWXL (Tosoh Bioscience) size exclusion column using phosphate buffer (pH 7.2). The column was connected to an HPLC system fitted with a RID detector (Shimadzu) and coupled to multiangle light scattering (DAWN) and quasi elastic light scattering detectors (Wyatt Technology). The molar mass (M_w), polydispersity index (PDI), and hydrodynamic radius (R_h) of the wild-type and mutant protein samples were determined using ASTRA (5.1.5) developed by Wyatt Technology. This software calculates the mass of a protein in each slice of the chromatogram and averages it; this value is reported as a molar mass average. It also provides the mass at the RI peak apex where the protein concentration is maximal.

Circular Dichroism (CD) Measurements. To investigate the secondary and tertiary structure of αA-wt crystallin and mutants, their far- and near-UV CD spectra were recorded at room temperature with a Jasco 715 spectropolarimeter. Protein concentrations of 0.1 and 1 mg/mL in 50 mM phosphate buffer (pH 7.0) were used for recording far- and near-UV spectra, with 0.1 and 1 cm path length quartz cells, respectively. The reported CD spectra are the average of five accumulations, which were smoothed and corrected for buffer

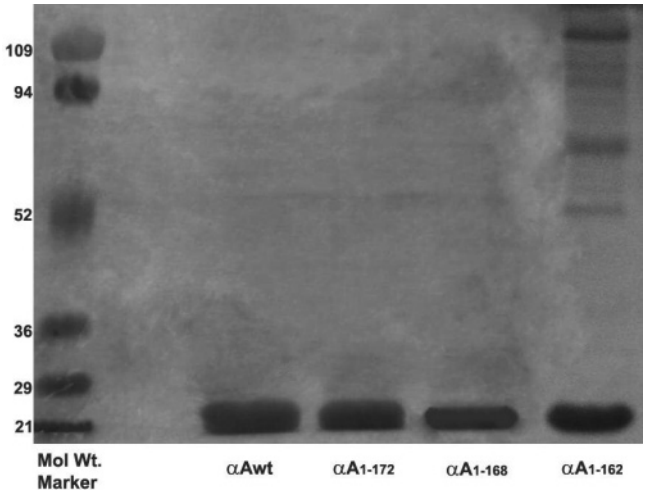

FIGURE 1: SDS−polyacrylamide gel electrophoresis of purified human αA-wt and its truncated mutants. Purification of the wild type and truncated mutants was done by a two-step size exclusion chromatography (see Experimental Procedures).

blanks. Secondary structure parameters were estimated with PROSEC derived from Yang et al. (*42*).

Chaperone Activity Measurements. Chaperone activity was assayed as described previously (*38*) by assessing the ability of the αA-wt and its truncated mutants to prevent (1) EDTA-induced aggregation of alcohol dehydrogenase (ADH) at 37 °C, (2) DTT-induced aggregation of insulin at 37 °C, and (3) heat denaturation of βL-crystallin at 62 °C. The aggregation of the target protein was monitored as light scattering at 360 nm as a function of time in a Shimadzu (Columbia, MD) UV160 spectrophotometer equipped with a temperature-regulated cell holder. The human αA:target protein ratios were 1:1 (64 and 64 μg) and 1:5 (12.8 and 64 μg) for the ADH assay, 1:1 (100 and 100 μg) and 1:2 (50 and 100 μg) for the insulin assay, and 1:10 (6.5 and 65 μg) and 1:20 (3.25 and 65 μg) for the βL-crystallin assay.

Determination of the Protein Stability of αA-wt and Its Truncated Mutants. The heat stability of the protein solutions (1.0 mg/mL) in 50 mM phosphate buffer (pH 7.4) was measured at 25, 37, and 62 °C (the later two temperatures were chosen because the chaperone assays were conducted at these temperatures) by monitoring light scattering at 360 nm for 30 min in the absence of target protein.

TNS [2-(p-Toluidino)naphthalene-6-sulfonic Acid] Binding Studies. The fluorescence of TNS (Marker Gene Technologies, Inc.) was measured with a RF-5301 PC spectrofluorophotometer from Shimadzu. To 1 mL of protein solution (0.1 mg/mL) in 50 mM phosphate buffer (pH-7.4) was added 5 μL of 20 mM TNS in DMSO (dimethyl sulfoxide), and the mixture was then incubated at 37 °C for 2.0 h. The fluorescence of TNS was measured using an excitation wavelength of 320 nm and an emission range of 350−550 nm to study the surface hydrophobicity of human αA-wt and its truncated mutants.

RESULTS

Purified Recombinant αA-Crystallin and Its Truncated Mutants. Wild-type and truncated αA-crystallin mutants were purified by two-step size exclusion chromatography, first by Sephacryl S-300 HR size exclusion columns (90 cm × 1.6 cm) followed by molecular sieve HPLC. The recovery of

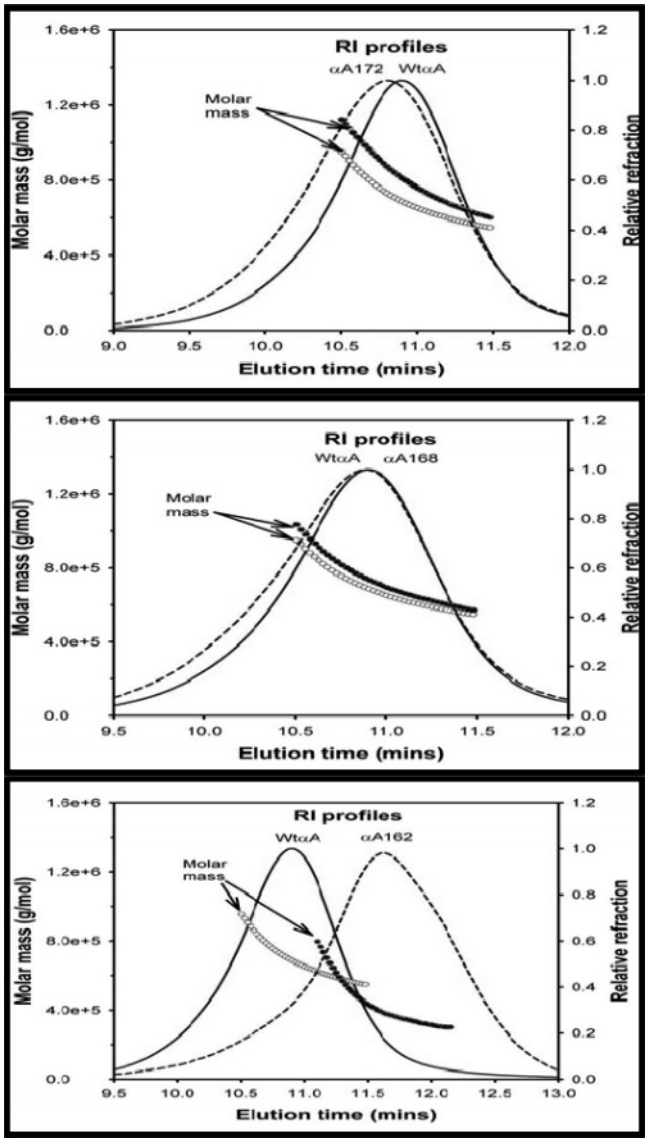

FIGURE 2: Overlay of molecular mass vs elution time of human αA-wt (○) and its truncated mutants (●) as determined by dynamic light scattering measurements. The molecular mass vs time plot showed evidence of a polydisperse nature.

the proteins varied from 30 to 10 mg from 1 L of expression medium. The purity of the proteins was confirmed by SDS−PAGE (Figure 1). Each purified protein, i.e., αA-wt, αA_{1-172}, αA_{1-168}, and αA_{1-162}, contains a prominent ~20 kDa band (Figure 1). It appears that αA-wt, αA_{1-172}, and αA_{1-168} are nearly 100% pure, whereas the αA_{1-162} fraction contains some contamination with presumably bacterial proteins (approximately less than 5%).

Quaternary Structural Parameters of Wild-Type αA-Crystallin and Truncated Mutants Determined by Dynamic Light Scattering. Figure 2 shows the size exclusion chromatograms of αA-wt superimposed with those of αA_{1-172}, αA_{1-168}, and αA_{1-162} showing refractive index (RI) profiles (reflective of protein concentration) and molar mass values [computed from light scattering (LS) and RI values]. Analysis of the RI peaks reveals that the molecular mass of αA_{1-172} is higher and that of αA_{1-162} is lower than that of αA-wt. The mass distribution of αA_{1-168} across the RI peak was very similar to that of αA-wt. The molar mass at the forefront of the chromatogram of αA-wt and all the three truncated

Table 1: Quaternary Structural Parameters of Wild-Type αA-Crystallin and Its Truncated Mutants Using Light Scattering Measurements[a]

protein	molar mass (M_w) average (g/mol)	molar mass (M_w) at the RI peak apex (g/mol)	polydispersity index (PDI)	hydrodynamic radius moments (nm) at RI peak (R_h)
wild-type α**A**	7.02×10^5	$(6.90 \pm 0.02) \times 10^5$	1.044 (0.5%)	8.5 ± 0.2
α$\mathbf{A}_1$−172	8.66×10^5	$(8.68 \pm 0.03) \times 10^5$	1.030 (0.6%)	9.3 ± 0.2
α$\mathbf{A}_1$−168	7.40×10^5	$(7.46 \pm 0.02) \times 10^5$	1.021 (0.4%)	8.5 ± 0.2
α$\mathbf{A}_1$−162	4.08×10^5	$(3.89 \pm 0.01) \times 10^5$	1.067 (0.5%)	8.6 ± 0.3

[a] The data acquired from RI and DAWN-QELS detectors were analyzed using ASTRA (5.1.5) developed by Wyatt Technologies. The percentage of deviation is given in parentheses.

mutants is significantly larger than at the back end of the chromatogram which indicates their polydisperse nature. Polydispersity depends on the distribution of masses across the peak. If the slope of the mass distribution line is steeper, it indicates a higher polydispersity. The polydispersity index (PDI) is above 1.00 in αA-wt, and the values vary between 1.021 and 1.067 in all the mutants (Table 1). The PDI of αA_{1-172} (1.030) is smaller than that of αA-wt (1.044),

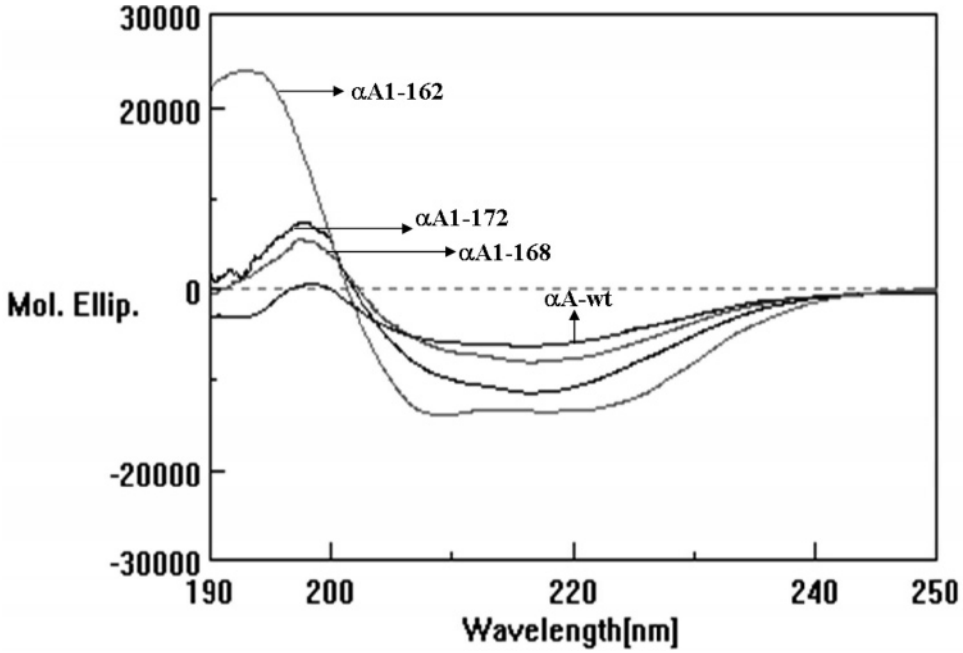

FIGURE 3: Far-UV CD spectra of human αA-wt and its truncated mutants recorded at room temperature. The protein concentration was 0.1 mg/mL, and the cell path length was 1.0 mm. The reported CD spectra are the average of smoothed five scans.

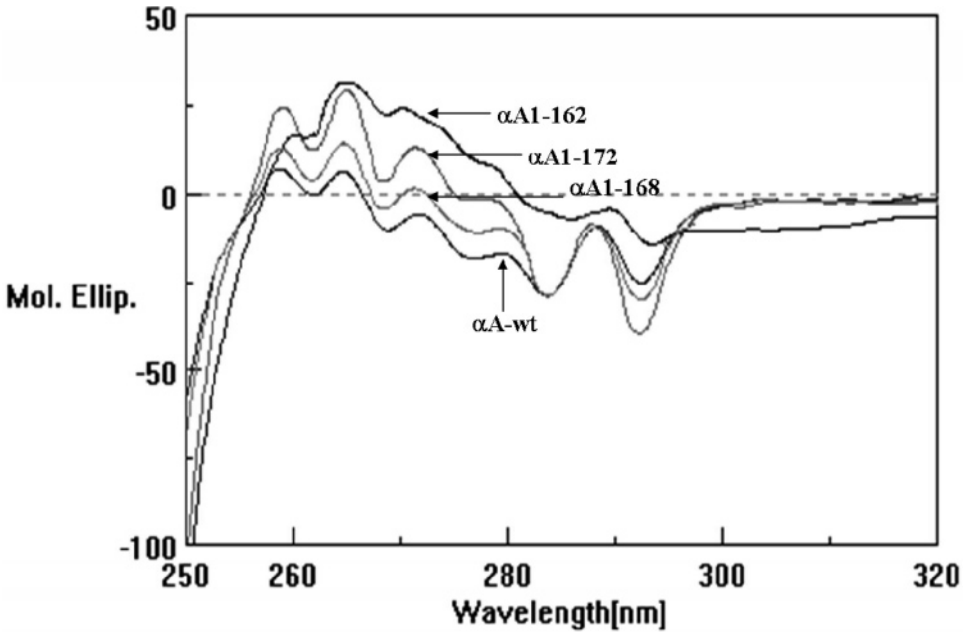

FIGURE 4: Near-UV CD spectra of human αA-wt and its truncated mutants recorded at room temperature. The reported CD spectra are the average of five smoothed scans. The protein concentration was 1.0 mg/mL, and the cell path length was 10.00 mm.

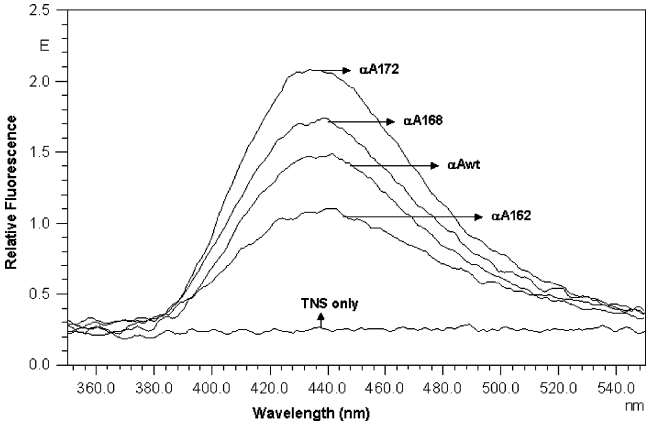

FIGURE 5: Fluorescence emission spectra of TNS-bound human αA-wt and its truncated mutants. The excitation wavelength was fixed at 320 nm and emission scanned between 350 and 550 nm. The protein concentration was 0.1 mg/mL in 50 mM phosphate buffer (pH 7.4).

although the slope of the mass distribution of the former is steeper (Figure 2). The first half of the RI peak of αA_{1-172} exhibits a higher polydispersity, whereas the second half exhibits less polydispersity than αA-wt. Since the majority of the mass is distributed in the second half of the αA_{1-172} peak, the PDI of the entire peak becomes smaller. The quaternary structural parameters of the αA-wt and the truncated mutants are summarized in Table 1. αA_{1-172} has the highest molecular mass average (866 kDa), and αA_{1-162} has the lowest average molecular mass (408 kDa). αA-wt (702 kDa) and αA_{1-168} (740 kDa) have almost similar molecular masses. Despite significant polydispersity, the molecular mass values at the RI peak are essentially the same as the average molecular mass values. The hydrodynamic radius moments do not vary significantly among the αA-wt and truncated αA crystallins except in αA_{1-172} which exhibits a 10% increase.

Conformational Studies. The far-UV and near-UV CD spectra of human αA-wt and the truncated mutants recorded at room temperature are shown in Figures 3 and 4, respectively. The spectra show that the secondary structures of αA-wt, αA_{1-172}, and αA_{1-168} are very similar. αA_{1-162} seems to have a higher content of α-helix. The levels of the various secondary structural elements (data not shown), as computed by PROSEC, confirmed this. As expected, the β-conformation constituted the major secondary structural component (~50−60%) of αA-crystallin (*43*). The α-helix content was increased by ~3-fold in αA_{1-162} accompanied by a loss of β-conformation and a concomitant increase in random coil conformation content. The difference in the near-UV CD spectra arises from the aromatic amino acids as well as from the folding of secondary structural components and their interaction within the compact protein structure. The near-UV spectrum of αA_{1-162} was very different from that of αA-wt and lacks all the distinct characteristics due to Trp, Tyr, and Phe accompanied by a significantly positive molecular ellipticity which is an indication of substantially

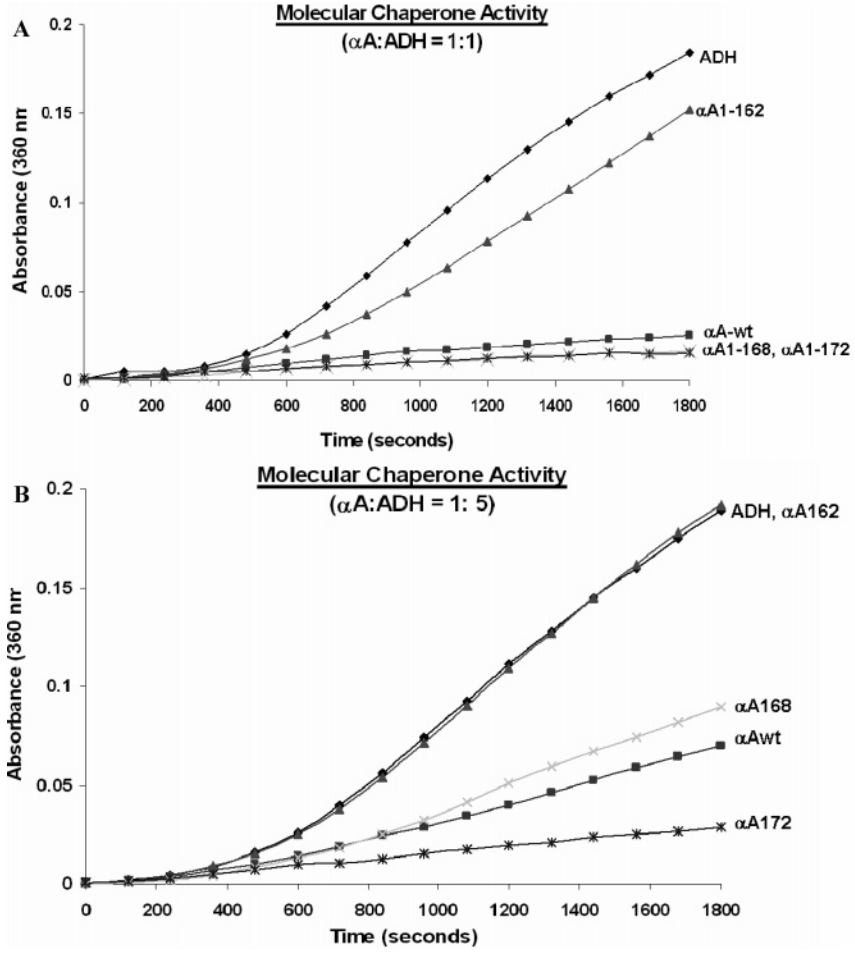

FIGURE 6: Chaperone activity of human αA-wt and its truncated mutants at 37 °C using alcohol dehydrogenase (ADH) in the presence of EDTA, with the αA:ADH ratios being (A) 1:1 and (B) 1:5 (the concentration of ADH is constant).

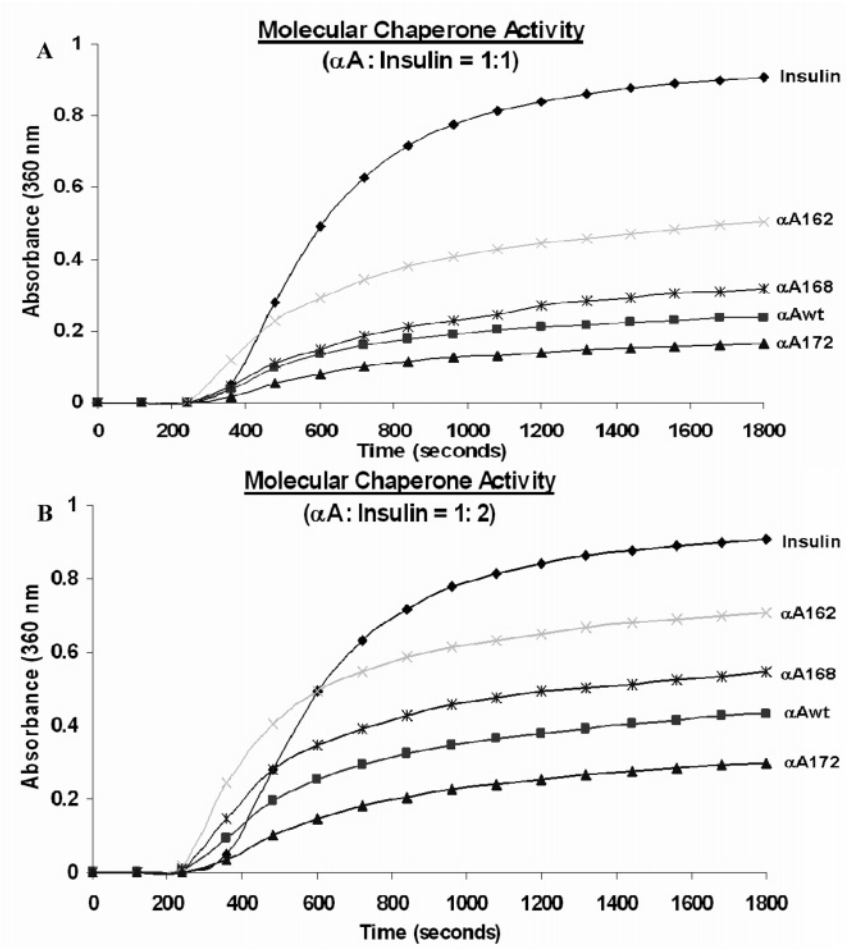

FIGURE 7: Chaperone activity of human αA-wt and its truncated mutants at 37 °C using insulin as the target protein in the presence of DTT, with the αA:insulin ratios being (A) 1:1 and (B) 1:2 (the concentration of insulin is constant).

altered tertiary structure. The near-UV CD spectrum of αA_{1-168} indicates a similarity of tertiary structure with αA-wt. αA_{1-172} shows distinct Trp, Tyr, and Phe signals but has a more positive molar ellipticity which may suggest a tertiary structure different from that of αA-wt and αA_{1-168}.

TNS [2-(p-Toluidino)naphthalene-6-sulfonic Acid] Binding Studies. To study the relative surface hydrophobicity of the truncated mutants of αA-Crystallin, TNS fluorescence spectra were monitored by using an RF-5301 PC spectrofluorophotometer (Shimadzu). TNS is a hydrophobic molecule and when bound to the hydrophobic sites present on the surface of a protein becomes highly fluorescent. Figure 5 shows the fluorescence spectra of TNS only and when it is bound to αA-wt and its truncated mutants. The highest fluorescence intensity was exhibited by αA_{1-172} followed by αA_{1-168} and αA-wt, while the intensity was substantially decreased in αA_{1-162}. Thus, the relative availability of the hydrophobic sites on the surface of the different truncated proteins, as shown by the spectra, is as follows: $\alpha A_{1-172} > \alpha A_{1-168} >$ αA-wt $> \alpha A_{1-162}$.

Chaperone Activity of αA-wt and Truncated Mutants. The chaperone activity was determined by in vitro assays using ADH in the presence of EDTA at 37 °C, insulin in the presence of DTT at 37 °C, and *β*L-crystallin at 62 °C as the target protein with two different proportions of αA: target protein (panels A and B of Figures 6−8, respectively). (1) In the ADH assay, at a 1:1 ratio of αA to ADH, αA-wt, αA_{1-172}, and αA_{1-168} were able to suppress completely the aggregation of ADH, the αA_{1-172} and αA_{1-168} mutants being slightly (∼5−6%) better chaperones than αA-wt (Figure 6A). The αA_{1-162} mutant, however, exhibited an 80% loss in chaperone activity as compared to that of αA-wt (Figure 6A). At an αA:ADH ratio of 1:5 (Figure 6B), αA_{1-162} completely lost the chaperone activity while αA_{1-168} exhibited a 16.6% loss of chaperone activity. The most interesting observation was made for αA_{1-172} which was able to suppress the aggregation of ADH nearly 35% better than αA-wt. (2) In the insulin assay, at a 1:1 ratio of αA to insulin (Figure 7A), the αA_{1-168} and αA_{1-162} mutants lost 11.6 and 40% chaperone activity, respectively, as compared to that of the wild type while αA_{1-172} exhibited 11.1% better chaperone activity. At an αA:insulin ratio of 1:2, αA_{1-162} exhibited an 80% loss of the chaperone activity while αA_{1-168} exhibited a 24% loss of chaperone activity. However, αA_{1-172} exhibited 28% better chaperone activity compared to that of the wild type (Figure 7B). (3) In the *β*L-crystallin assay, at a 1:10 ratio of αA to *β*L, αA-wt, αA_{1-172}, and αA_{1-168} completely suppressed *β*L thermal aggregation at 62 °C whereas αA_{1-162} had no chaperone activity (Figure 8A). At an αA:*β*L-crystallin ratio of 1:20, αA_{1-168} exhibited a 12% loss of activity, αA_{1-162} lacked any chaperone activity, and αA_{1-172} exhibited 46% better chaperone activity than the wild type (Figure 8B). Thus, all the three assays showed αA_{1-172} having significantly better chaperone activity than αA-wt as summarized by the bar chart in Figure 9.

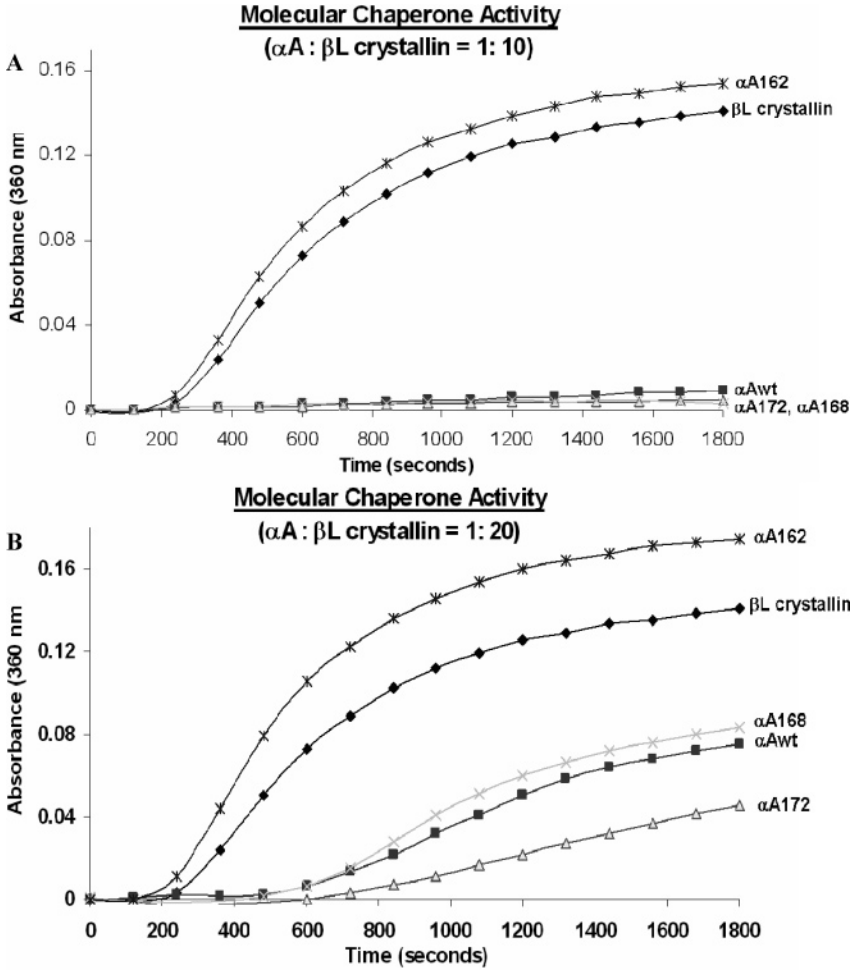

FIGURE 8: Chaperone activity of human αA-wt and its truncated mutants using *β*L-crystallin as the target protein at 62 °C with the αA: *β*L-crystallin ratios being (A) 1:10 and (B) 1:20 (the concentration of *β*L is constant).

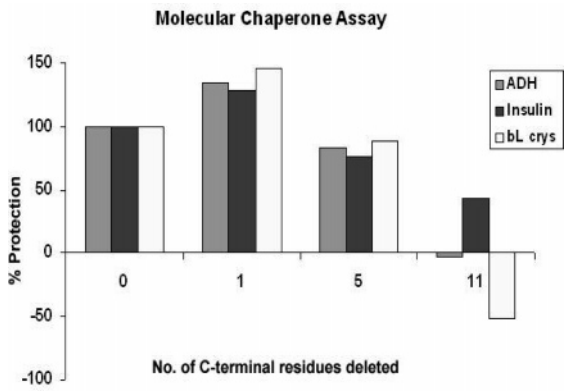

FIGURE 9: Summary of the chaperone assay data for human αA-wt and its truncated mutants (expressed as the percentage protection of target proteins, i.e., ADH, insulin, and *β*L-crystallin from denaturation). Chaperone activity values at 1800 s were taken from Figures 6B, 7B, and 8B.

Heat Stability of αA-wt and Its Truncated Mutants. By monitoring light scattering at 25, 37, and 62 °C, we determined the heat stability of the human αA-wt and its truncated mutants. The data are presented in Figure 10. At 25 °C, the wild type and the mutants showed no evidence of any denaturation and aggregation. At 37 °C, the stability of αA-wt, αA_{1-172}, and αA_{1-168} was not affected while αA_{1-162} exhibited some degree of aggregation toward the end of the incubation period. At 62 °C, αA-wt, αA_{1-172}, and αA_{1-168} were stable whereas αA_{1-162} exhibited excessive aggregation due to complete denaturation.

DISCUSSION

As a member of the small heat shock protein family, α-crystallin exhibits chaperone-like function and protects structurally compromised proteins, thus increasing the overall cellular tolerance of lens against stress. Because of its functional importance, the impact of the post-translational modifications of α-crystallin has been extensively studied. Of the many reported post-translational modifications, truncation of amino acids from the C-terminal region is the major modification occurring in αA-crystallin. In human lenses, C-terminal cleavage of αA-crystallin at residues 101, 151, 162, 168, and 172 has been reported (*24*, *32*−*34*). Because the role that each of these truncated forms of αA-crystallin may play in the lens function is not known, we have cloned, overexpressed, and characterized the structure and function of human αA-wt and the C-terminally truncated mutants.

The major focus of this study is the structure, oligomeric size, and chaperone function of αA_{1-172} formed by the enzymatic cleavage of the serine residue at the C-terminus of αA-crystallin which constitutes 30−50% of the total αA-crystallin in human lenses (*37*). The oligomeric size of this protein has been determined by the dynamic light scattering method. The molar mass average value is 8.66 e^5 or 866

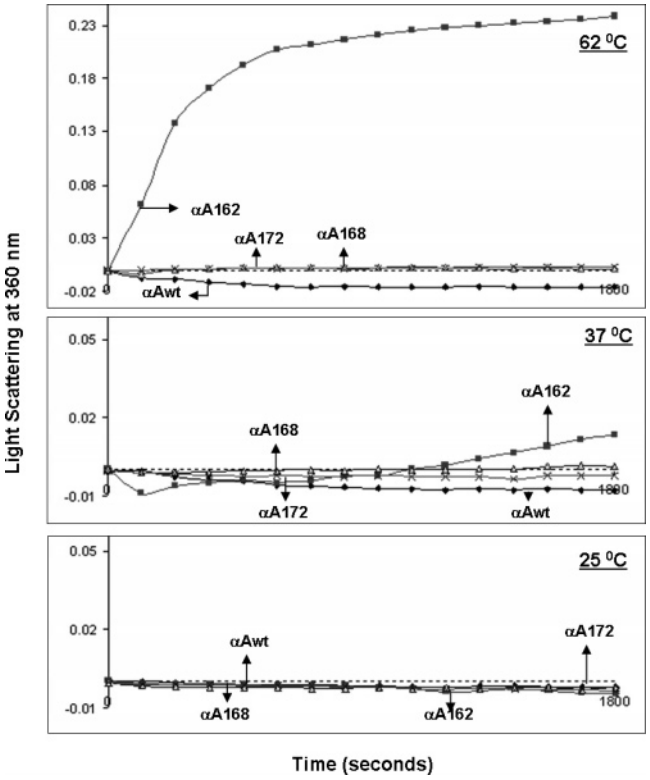

FIGURE 10: Heat stability curves for human αA-wt and its truncated mutants at 25, 37, and 62 °C. Light scattering was recorded at 360 nm for 1800 s.

kDa, and the value at the RI peak is 8.68 e^5 or 868 kDa as shown in Table 1 as opposed to 7.02 (702 kDa) and 6.9 e^5 (690 kDa) for αA-wt, respectively; the αA_{1-172} truncated protein is 23.4% larger than αA-wt. The only obvious structural difference which can explain this mass difference is evident only in the near-UV spectrum (Figure 4). The near-UV spectrum reveals the microenvironment changes for aromatic amino acids, Trp, Tyr, and Phe. αA-wt exhibited a spectrum which was expected from earlier studies (*46*). Although all the spectral signals due to Trp, Tyr, and Phe are distinctly evident in αA_{1-172}, the molar ellipticity is more positive which indicates some changes in tertiary structure. However, it is uncertain here whether these structural changes cause αA_{1-172} to aggregate to a more stable higher-molecular mass protein.

It remains to be shown whether the cleavage of the $Ser_{172}-Ser_{173}$ bond is regulated, how it is regulated, and whether αA_{1-172} with improved chaperone activity has a well-defined biological role. An earlier study provided data suggestive of a developmentally regulated process in which a protease specific for the Ser−Ser bond is induced or activated in the eye lens within the early years of life (*37*). Similar protease activity has been reported to be present in bovine lens extract (*47*). An age-dependent cleavage of the C-terminal residue has been reported in the fetal versus adult bovine lenses (*25*). A 2-fold increase in the levels of αA_{1-172} was observed in diabetic human lenses as compared to age-matched control lenses (*36*). It appears that this occurs under increased oxidative stress where proteins undergo oxidation and aggregation; formation of αA_{1-172} will be a biological response to increased oxidative stress in diabetes, thus supporting metabolic regulation of the cleavage of the C-terminal Ser−Ser bond. In both aging and diabetes, an increased level of lens protein aggregation is expected, and thus, it is advantageous to have a more active molecular chaperone. Interestingly, cleavage of the C-terminal Ser residue produces an αA-crystallin, i.e., αA_{1-172}, functionally more active than αA-wt. In fact, we have convincingly shown this by choosing three different target proteins (ADH, insulin, and βL-crystallin) and two different temperatures (37 and 62 °C) for determining chaperone activity (Figures 6−9). For each assay method, two proportions of αA to target protein (1:1 and 1:5 for ADH, 1:1 and 1:2 for insulin, and 1:10 and 1:20 for βL-crystallin) were used. The chaperone activity of αA_{1-172} was ~28−46% higher than that of αA-wt when higher proportions were used, whereas at lower proportions, as expected, the chaperone activity was only 3−11% higher. The strongest explanation for the behavior of the αA_{1-172} mutant as a better chaperone comes from the study with the hydrophobic probe, TNS, which shows the strongest binding of TNS (highest relative fluorescence) to

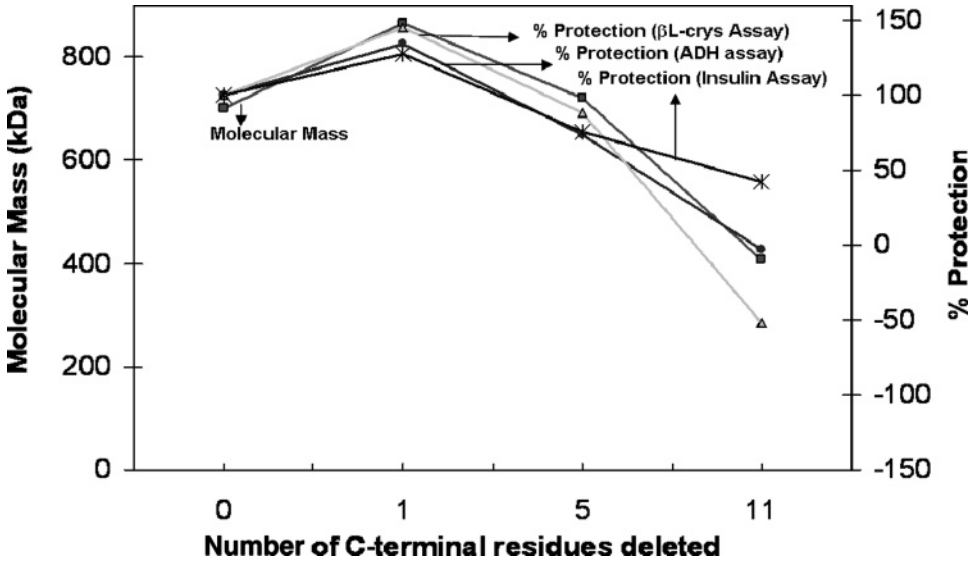

FIGURE 11: Relationship between oligomeric size and chaperone activity (expressed as the percentage protection of target proteins, i.e., βL-crystallin, ADH, and insulin denaturation). Molecular mass values were taken from Figure 1, and chaperone activity values at 1800 s were taken from Figures 6B, 7B, and 8B ($r^2 = 0.949$ for ADH, $r^2 = 0.878$ for insulin, and $r^2 = 0.981$ for βL-crystallin).

the available hydrophobic sites which can be directly correlated to the exposed hydrophobic sites for the target protein binding (Figure 5). TNS fluorescence data also show that the conformation of αA_{1-172} is different from that of αA-wt, αA_{1-168}, and αA_{1-162}.

Apart from αA_{1-172}, we have characterized two other truncated αA-crystallins, αA_{1-168} and αA_{1-162}, which have been reported to be present in human lens homogenates, although in relatively small amounts (*32*−*34*). However, mass spectrometric analysis of human lens water soluble protein showed no evidence of these truncated αA-crystallins (*36*). The structure and oligomeric size of αA_{1-168} exhibited a strong similarity to those of αA-wt, but the chaperone activities were nearly the same or slightly lower depending on the assay method and the αA:target protein proportion. The αA_{1-168} mutant has been characterized in two earlier studies (*31*, *48*). In the first study by Thampi and Abraham (2003), the chaperone activity of rat αA_{1-168} was slightly better than that of αA-wt. In the same study, αA_{1-172}, which is not known to exist in rat lens, exhibited slightly improved chaperone activity and the molecular mass was unchanged. In a subsequent study by Aquilina et al. (*48*), αA_{1-168} (from an unknown source) had slightly decreased molecular mass and chaperone activity.

On the basis of our earlier studies with truncated rat αA-crystallins, a decrease in the oligomeric size as well as chaperone activity of the truncated αA_{1-162} mutant was expected (*31*). However, there are distinct differences between rat and human αA_{1-162}. While the oligomeric size of rat αA_{1-162} was 150 kDa, human αA_{1-162} had an oligomeric size of nearly 400 kDa (Figure 2 and Table 1). The reason for this difference is unclear. However, it can be suggested that this difference is due to the presence of two cysteine residues (Cys_{131} and Cys_{142}) in human αA-crystallin as compared to only Cys_{131} in rat αA-crystallin. It is known that these two cysteines are susceptible to oxidation and formation of intramolecular and intermolecular disulfide bonds (*33*, *44*, *45*). It is also noteworthy that αA_{1-162} is heat unstable and was completely denatured at high temperatures, i.e., 62 °C as shown in Figure 10. This could be one of the reasons for the absorbance of the αA_{1-162}−βL-crystallin complex being higher than that of βL-crystallin alone in the βL assay (Figure 8A,B). Even at 37 °C, it showed slight aggregation relative to αA-wt and other truncated mutants as shown by the increase in the absorbance at 360 nm after 1100 s (Figure 10). Thus, in αA_{1-162}, heat stability could be a factor which could directly influence chaperone activity.

In Figure 11, we have compared the chaperone activity (expressed as percentage protection) with the molecular masses of the truncated mutants. There is significantly positive correlation between the chaperone-like function ($r^2 = 0.949$ for ADH, $r^2 = 0.878$ for insulin, and $r^2 = 0.981$ for βL-crystallin) and the oligomeric size. With the decreasing molecular mass, the chaperone-like activity also decreases, and in the case of αA_{1-172}, an increase in oligomeric size by 23.36% shows an increase in chaperone activity of ∼28−46%. Such a relationship between oligomeric mass and chaperone activity was reported for rat αA-crystallin truncated mutants (*31*). However, the influence of structural changes on chaperone activity cannot be ruled out. On the other hand, structure is expected to influence oligomerization which in turn can influence chaperone function.

It is unclear why the cleavage of one amino acid residue, namely Ser_{173}, from the C-terminus causes aggregation of αA-crystallin, forming oligomers with a molecular mass higher than that of αA-wt. The only structural change which can be correlated to this is an increase in molar ellipticity in the near-UV spectrum (Figure 4), which indicates that the tertiary fold is slightly different in the αA_{1-172} mutant. The change in the oligomeric structure resulted in increased chaperone activity presumably due to an increased level of exposure of target protein binding sites, as shown by enhanced surface hydrophobicity (Figure 5). It is also noteworthy that in an earlier study, Cho and Abraham (*49*) have reported increased chaperone activity in human αB-crystallin after the cleavage of the five C-terminal residues. However, there was no evidence of an increased level of aggregation of this truncated αB-crystallin mutant.

REFERENCES

1. Bloemendal, H. (1977) The vertebrate eye lens, *Science 19* (4299), 127−138.
2. Bloemendal, H. (1981) *Molecular and Cellular Biology of the Eye Lens*, pp 1−47, John Wiley and Sons, New York.
3. Veretout, F., Delaye, M., and Tardieu, A. (1989) Molecular basis of eye lens transparency. Osmotic pressure and X-ray analysis of α-crystallin solutions, *J. Mol. Biol. 205* (4), 713−728.
4. de Jong, W. W., Caspers, G. J., and Leunissen, J. A. (1998) Genealogy of the α-crystallin−small heat-shock protein super family, *Int. J. Biol. Macromol. 22* (3−4), 151−162.
5. Van Der Ouderaa, F. J., De Jong, W. W., Hilderink, A., and Bloemendal, H. (1974) The amino-acids sequence of the αB2 chain of bovine α-crystallin, *Eur. J. Biochem. 49* (1), 157−168.
6. Van der Ouderaa, F. J., de Jong, W. W., and Bloemendal, H. (1973) The amino-acid sequence of the αA2 chain of bovine α-crystallin, *Eur. J. Biochem. 39* (1), 207−222.
7. Ingolia, T. D., and Craig, E. A. (1982) Four small *Drosophila* heat shock proteins are related to each other and to mammalian α-crystallin, *Proc. Natl. Acad. Sci. U.S.A. 79* (7), 2360−2364.
8. Horwitz, J. (1992) α-Crystallin can function as a molecular chaperone, *Proc. Natl. Acad. Sci. U.S.A. 89* (21), 10449−10453.
9. Wistow, G. (1985) Domain structure and evolution in α-crystallins and small heat-shock proteins, *FEBS Lett. 181*, 1−6.
10. Caspers, G. J., Leunissen, J. A., and de Jong, W. W. (1995) The expanding small heat-shock protein family, and structure predictions of the conserved "α-crystallin domain", *J. Mol. Evol. 40* (3), 238−248.
11. Wistow, G. (1985) Domain structure and evolution in α-crystallins and small heat-shock proteins, *FEBS Lett. 181* (1), 1−6.
12. Kokke, B. P., Leroux, M. R., Candido, E. P., Boelens, W. C., and de Jong, W. W. (1998) *Caenorhabditis elegans* small heat-shock proteins Hsp12.2 and Hsp12.3 form tetramers and have no chaperone-like activity, *FEBS Lett. 433* (3), 228−232.
13. Leroux, M. R., Ma, B. J., Batelier, G., Melki, R., and Candido, E. P. (1997) Unique structural features of a novel class of small heat shock proteins, *J. Biol. Chem. 272* (19), 12847−12853.
14. Leroux, M. R., Melki, R., Gordon, B., Batelier, G., and Candido, E. P. (1997) Structure-function studies on small heat shock protein oligomeric assembly and interaction with unfolded polypeptides, *J. Biol. Chem. 272* (39), 24646−24656.
15. Van Kleef, F. S., De Jong, W. W., and Hoenders, H. J. (1975) Stepwise degradations and deamidation of the eye lens protein α-crystallin in ageing, *Nature 258* (5532), 264−266.
16. Van den Oetelaar, P. J., and Hoenders, H. J. (1989) Folding-unfolding and aggregation-dissociation of bovine α-crystallin subunits: Evidence for unfolding intermediates of the αA subunits, *Biochim. Biophys Acta 995* (1), 91−96.
17. Merck, K. B., De Haard-Hoekman, W. A., Oude Essink, B. B., Bloemendal, H., and De Jong, W. W. (1992) Expression and aggregation of recombinant αA-crystallin and its two domains, *Biochim. Biophys. Acta 1130* (3), 267−276.
18. Carver, J. A., and Lindner, R. A. (1998) NMR spectroscopy of α-crystallin. Insights into the structure, interactions and chaperone action of small heat-shock proteins, *Int. J. Biol. Macromol. 22* (3−4), 197−209.

19. Narberhaus, F. (2002) α-Crystallin-type heat shock proteins: Socializing minichaperones in the context of a multichaperone network, *Microbiol. Mol. Biol. Rev. 66* (1), 64−93.
20. Carver, J. A. (1999) Probing the structure and interactions of crystallin proteins by NMR spectroscopy, *Prog. Retinal Eye Res. 18* (4), 431−462.
21. Kramps, J. A., de Jong, W. W., Wollensak, J., and Hoenders, H. J. (1978) The polypeptide chains of α-crystallin from old human eye lenses, *Biochim. Biophys. Acta 533* (2), 487−495.
22. Groenen, P. J., Merck, K. B., de Jong, W. W., and Bloemendal, H. (1994) Structure and modifications of the junior chaperone α-crystallin. From lens transparency to molecular pathology, *Eur. J. Biochem. 225* (1), 1−19.
23. Takemoto, L., and Gopalakrishnan, S. (1994) αA-Crystallin: Quantitation of C-terminal modification during lens aging, *Curr. Eye Res. 13* (12), 879−883.
24. Takemoto, L. J. (1995) Identification of the in vivo truncation sites at the C-terminal region of α-A crystallin from aged bovine and human lens, *Curr. Eye Res. 14* (9), 837−841.
25. Emmons, T., and Takemoto, L. (1992) Age-dependent loss of the C-terminal amino acid from α-crystallin, *Exp. Eye Res. 55* (4), 551−554.
26. Takemoto, L., Emmons, T., and Horwitz, J. (1993) The C-terminal region of α-crystallin: Involvement in protection against heat-induced denaturation, *Biochem. J. 294* (Part 2), 435−438.
27. Kelley, M. J., David, L. L., Iwasaki, N., Wright, J., and Shearer, T. R. (1993) α-Crystallin chaperone activity is reduced by calpain II in vitro and in selenite cataract, *J. Biol. Chem. 268* (25), 18844−18849.
28. Smulders, R. H. P. H., Carver, J. A., Lindner, R. A., van Boekel, M. A., Bloemendal, H., and de Jong, W. W. (1996) Immobilization of the C-terminal extension of bovine αA-crystallin reduces chaperone-like activity, *J. Biol. Chem. 271* (46), 29060−29066.
29. Andley, U. P., Mathur, S., Griest, T. A., and Petrash, J. M. (1996) Cloning, expression, and chaperone-like activity of human αA-crystallin, *J. Biol. Chem. 271* (50), 31973−31980.
30. Pasta, S. Y., Raman, B., Ramakrishna, T., and Rao, Ch. M. (2002) Role of the C-terminal extensions of α-crystallins. Swapping the C-terminal extension of α-crystallin to αB-crystallin results in enhanced chaperone activity, *J. Biol. Chem. 277* (48), 45821−45828.
31. Thampi, P., and Abraham, E. C. (2003) Influence of the C-terminal residues on oligomerization of αA-crystallin, *Biochemistry 42* (40), 11857−11863.
32. Colvis, C., and Garland, D. (2002) Posttranslational modification of human αA-crystallin: Correlation with electrophoretic migration, *Arch. Biochem. Biophys. 397* (2), 319−323.
33. Lund, A. L., Smith, J. B., and Smith, D. L. (1996) Modifications of the water-insoluble human lens α-crystallins, *Exp. Eye Res. 63* (6), 661−672.
34. Ma, Z., Hanson, S. R., Lampi, K. J., David, L. L., Smith, D. L., and Smith, J. B. (1998) Age-related changes in human lens crystallins identified by HPLC and mass spectrometry, *Exp. Eye Res. 67* (1), 21−30.
35. Miesbauer, L. R., Zhou, X., Yang, Z., Yang, Z., Sun, Y., Smith, D. L., and Smith, J. B. (1994) Post-translational modifications of water-soluble human lens crystallins from young adults, *J. Biol. Chem. 269* (17), 12494−12502.
36. Thampi, P., Hassan, A., Smith, J. B., and Abraham, E. C. (2002) Enhanced C-terminal truncation of αA- and αB-crystallins in diabetic lenses, *Invest. Ophthalmol. Visual Sci. 43* (10), 3265−3272.
37. Takemoto, L. J. (1998) Quantitation of specific cleavage sites at the C-terminal region of α-A crystallin from human lenses of different age, *Exp. Eye Res. 66* (2), 263−266.
38. Bera, S., and Abraham, E. C. (2002) The αA-crystallin R116C mutant has a higher affinity for forming heteroaggregates with αB-crystallin, *Biochemistry 41* (1), 297−305.
39. Shroff, N. P., Bera, S., Cherian-Shaw, M., and Abraham, E. C. (2001) Substituted hydrophobic and hydrophilic residues at methionine-68 influence the chaperone-like function of αB-crystallin, *Mol. Cell. Biochem. 220* (1−2), 127−133.
40. Shroff, N. P., Cherian-Shaw, M., Bera, S., and Abraham, E. C. (2000) Mutation of R116C results in highly oligomerized αA-crystallin with modified structure and defective chaperone-like function, *Biochemistry 39* (6), 1420−1426.
41. Laemmli, U. K. (1970) Cleavage of structural proteins during the assembly of the head of bacteriophage T4, *Nature 227* (5259), 680−685.
42. Yang, J. T., Wu, C. S., and Martinez, H. M. (1986) Calculation of protein conformation from circular dichroism, *Methods Enzymol. 130*, 208−269.
43. Liang, J. N., Andley, U. P., and Chylack, L. T., Jr. (1985) Spectroscopic studies on human lens crystallins, *Biochim. Biophys. Acta 832*, 197−203.
44. Takemoto, L. (1996) Increase in the intramolecular disulfide bonding of α-A crystallin during ageing of the human lens, *Exp. Eye Res. 67*, 585−590.
45. Cherian-Shaw, M., Smith, J. B., Jiang, X. Y., and Abraham, E. C. (1999) Intrapolypeptide disulfides in human αA-crystallin and their effect on chaperone-like function, *Mol. Cell. Biochem. 199* (1−2), 163−167.
46. Sun, T. X., Das, B. K., and Liang, J. J. (1997) Conformational and functional differences between recombinant human lens αA- and αB-crystallin, *J. Biol. Chem. 272* (10), 6220−6225.
47. Sharma, K. K., Kester, K., and Elser, N. (1996) Identification of new lens protease(s) using peptide substrates having in vivo cleavage sites, *Biochem. Biophys. Res. Commun. 218* (1), 365−370.
48. Aquilina, J. A., Benesch, J. L., Ding, L. L., Yaron, O., Horwitz, J., and Robinson, C. V. (2005) Subunit exchange of polydisperse proteins: Mass spectrometry reveals consequences of αA-crystallin truncation, *J. Biol. Chem. 280* (15), 14485−14491.
49. Cho, W., and Abraham, E. C. (2002) C-Terminal truncation of five amino acid residues of αB-crystallin influences its chaperone function, ARVO Abstract B545.

BI0618722